Electrical Power and Energy Systems 159 (2024) 110025

Contents lists available at ScienceDirect

International Journal of Electrical Power and Energy Systems

journal homepage: www.elsevier.com/locate/ijepes

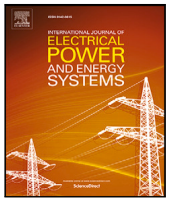

A scenario-based stochastic model predictive control approach for microgrid operation at an Australian cotton farm under uncertainties

Yunfeng Lin [a,*], Li Li [a], Jiangfeng Zhang [b], Jiatong Wang [a]

[a] School of Electrical and Data Engineering, University of Technology Sydney, Sydney, New South Wales, Australia
[b] Department of Automotive Engineering, Clemson University, Greenville, SC, USA

ARTICLE INFO

Keywords:
Cotton farm
Scenario-based
Microgrid
Renewable energy sources
Model predictive control
Water pumps

ABSTRACT

This study presents a scenario-based model predictive control (MPC) approach to minimize the cotton farm microgrid operational cost under uncertainties. Uncertainties in cotton farms may come from renewable energy generation, water demand, precipitation, and evaporation, so the cotton field pumping system operation can be formulated as a stochastic MPC problem to accommodate uncertain climate conditions and real-time changes in irrigation demand. Scenario generation and reduction techniques can obtain typical scenarios and their probabilities. The typical scenarios can be used in the MPC iterative step to facilitate modelling the proposed stochastic optimization problem. This study discusses static and dynamic uncertainty modelling techniques used for MPC, and each technique is analysed separately in grid-connected and islanded microgrids through case studies. In the grid-connected dynamic scenario-based MPC, the operational cost is AU$ 18,797 over the entire irrigation period, which is AU$ 8759 lower than that of the standard MPC. Furthermore, for the islanded dynamic scenario-based MPC, the operational cost is AU$ 24,443 over the entire irrigation period, which is AU$ 6721 lower than the standard MPC.

1. Introduction

Energy purchase costs grow very fast for cotton farms, where electricity and diesel consumption are a notable portion of the average cotton production costs [1]. This trend imposes a considerable financial burden on the cotton growers. Since 2000, Australian growers have experienced significant price increases in electricity costs, about 350% increase after removing the effect of the 45 ~ 50% accumulated inflation [2]. In [3], the authors explore the application of MGs in cotton farms and provide sustainable and cost-effective energy solutions for cotton farms. Thus, one of the ways by which cotton growers can reduce their direct energy operational costs is to introduce renewable energy and implement operational strategies to reduce direct energy consumption. Unlike conventional power generation, renewable energy (such as solar) is always intermittent, bringing significant uncertainties to power generation and scheduling [4]. This study aims to develop effective methods to reduce operating costs and maintain reliability under uncertainties from renewable energy sources and changing demand.

1.1. Literature review

In recent years, more and more literature has combined small-scale RES with traditional generator sets to establish the MG system, an emerging way to absorb RES on demand, e.g., Ref. [5] uses the energy management system to minimize the daily operating cost of the MG and maximize self-consumption of renewable energy sources. Therefore, the operational cost can be reduced by improving the utilization rate of renewable. MPC has advantageous features to operate MG owing to its capability to handle uncertainties [6]. Accordingly, MPC methods have been widely applied to MG operations. In [7], the MPC approach aims to optimize the power distribution among generators, load, and battery storage, ensuring stability and efficient management of the microgrid under varying conditions. In addition, Ref. [8] proposes an online optimal operation method for combined cooling, heating, and power MG systems based on MPC, compensating for prediction errors through two hierarchies of feedback correction. Furthermore, the MPC strategy in [9] minimizes the operational cost of the cotton farm MG system in Australia. The above studies emphasize the robustness of MPC and note that uncertainty will affect the results; however, the uncertainties are not modelled.

Many studies have discussed methods of generating appropriate scenarios to model uncertainty [10]. A nonlinear programming method based on scenario trees is proposed in [11], in order to generate a large number of scenarios and then reduce them to a limited number of discrete matrices as the typical scenario results. The authors in [12]

* Corresponding author.
E-mail address: Yunfeng.Lin@alumni.uts.edu.au (Y. Lin).

https://doi.org/10.1016/j.ijepes.2024.110025
Received 23 December 2022; Received in revised form 28 March 2024; Accepted 3 May 2024
Available online 13 May 2024

Nomenclature

Abbreviations

FIT	Feed-In Tariff
GMG	Grid-connected Microgrid
IMG	Islanded Microgrid
MG	Microgrid
MPC	Model Predictive Control
PV	Photovoltaic
RES	Renewable Energy Source
SOC	State of Charge
TDH	Total Dynamic Head

Indices

i	Index of pumps
s	Index of typical scenarios
t	Time index (h)

Parameters

$\delta^{in}_{diesel,i}$	Diesel consumption of the ith independent pump in IMG for lifting 1 ML water to 1 mTHD (L/ML/mTHD)
κ_d	Lead–acid battery degradation coefficient
C_{Bat}	Battery storage cost (AU$)
K or K^{in}	Number of MG pumps or independent pumps
$P^{in}_{pump,i}$	Rated power of ith independent pump in GMG (kW)
P^{max}_{fi}	Maximum power allowed to be fed into to the grid (kW)
$P^{MG}_{pump,i}$	Rated power of ith pump connected to microgrid (kW)
P^{total}_{pump}	Sum of all the pump's maximum rated power (kW)
W_{eva}	Hourly evaporation volume from reservoir (ML)
W_{irr}	Hourly cotton farm irrigation water volume (ML)
W_{R_res}	Hourly precipitation amount into the reservoir (ML)

Variables

ξ	Binary variable of the grid energy import or export
ξ_B	Binary variable of battery charge or discharge
P_{diesel}	Power generated by diesel generator (kW)
P_{fi}	Feed-in power to the grid (kW)
P_{grid}	Power purchased from grid (kW)
P_{solar}	PV power generation (kW)
P^{panel}_{solar}	Power output of a single PV panel (kW)
S^{SOC}	State of charge of battery storage (%)
x_i or x^{in}_i	Control variable for the pump's on/off state (kW)

present a stochastic programming method using scenario generation to deal with stochastic load and wind power uncertainty. Additionally, Ref. [13] considers price uncertainty and uses a piecewise linear approximation of degradation cost. Moreover, in [14], the energy storage system operation scheduling problem is formulated as a two-stage stochastic programming model based on the scenario-based method. In addition, several studies use scenario-based approaches to build stochastic models in MG operation studies. In [15], the uncertainty of RES output power and load demand forecast errors are modelled by scenario-based techniques for optimal energy management of MGs. An RES stochastic model is adopted in [16], which uses the scenario reduction process to convert the stochastic problem into many deterministic problems with different probabilities and then optimizes each deterministic problem. The above-mentioned literature focuses on mathematical algorithms, but the description of the uncertain phenomena and effects in the actual applications is limited.

On the other hand, scenario-based stochastic MPC has been applied to smart grid operation area [17]. Furthermore, Ref. [18] introduces different classifications of the available methods based on the dynamic characteristics of the system, management of the probabilistic constraints, feasibility, and the properties of convergence. Additionally, Ref. [19] provides an overview of the core concepts related to MPC and stochastic optimal control under uncertainties and discusses the disturbance estimation and the impact of the estimation quality on MPC performance. In [20], a scenario-based MPC approach is proposed through a data-driven machine learning method. Likewise, a scenario-based MPC controller is implemented in [21] for the management of building heating, ventilation, and air conditioning systems. Furthermore, a scenario-based model predictive operation control of rural area IMG is proposed in [22]. Also, in our previous work, a GMG under uncertainty is adopted for water pumps on an Australian cotton farm [23].

1.2. Research gaps and contributions

Nevertheless, the methods mentioned above do not accurately model the uncertainties from different sources and do not compare the impact of different uncertainty models on the optimization results for GMG and IMG. This study extends our previous study [9] and proposes two uncertainty models (i.e., static scenario-based and dynamic scenario-based uncertainty models) to assist the optimal operation of cotton farm MG under uncertainty during an irrigation period. Here, the static scenario-based uncertainty model refers to the case that the uncertainty dataset for scenario generation and reduction is fixed for the entire irrigation period, and the resultant typical scenarios are used for all the MPC iterations. Alternatively, in the dynamic scenario-based uncertainty model, the uncertainty dataset will be dynamically updated for scenario generation and reduction along with the moving time horizon within MPC; consequently, the corresponding typical scenarios are dynamically updated within each MPC iteration. After deciding the uncertainty scenarios using either the static or dynamic scenario-based methods, a stochastic MPC strategy is proposed for the above two uncertainty models. The demand and weather uncertainties on both GMG and IMG are also considered. This paper uses the SCENARD toolbox [24] based on the Kantorovich distance [24] method to deal with uncertainties. CPLEX 12.10 with MATLAB is used to solve the underlying optimization problems. Therefore, the novelties are to consider both static and dynamic scenario-based uncertainty models and their impact on cotton farm GMG and IMG.

The remaining part of this paper is organized as follows. Section 2 describes the cotton farm MG and scenario-based uncertainty models. Section 3 presents a case study to simulate the proposed methodology based on the actual data from a New South Wales cotton farm. Section 4 discusses the simulation results for each case, and Section 5 concludes the paper by highlighting the significant meaning of the main results.

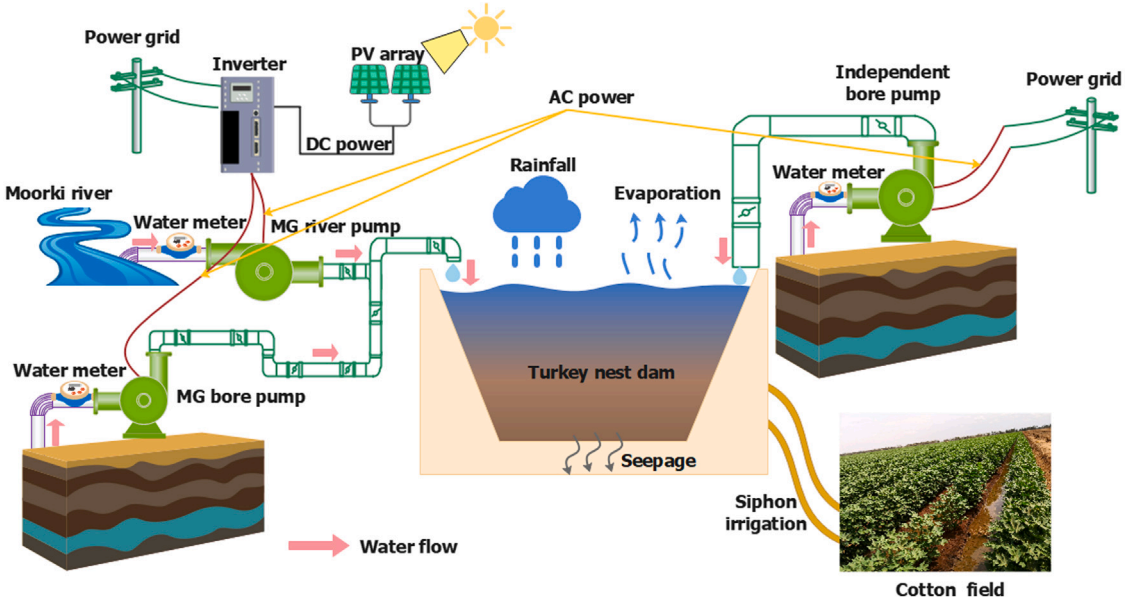

Fig. 1. Grid-connected cotton farm microgrid and pumping water system.

2. MPC of cotton farm microgrids and scenario-based uncertainty modelling

Based on the current situation of using hybrid RESs and the geographical location of general Australian cotton farms, the MG system in Australian cotton farms can be divided into GMG and IMG. Therefore, the following assumptions are used to model the studied cotton farm MG. Cotton farms have their own water storage system for irrigation and tailwater recovery. The pumps will pump water from the bore or river into the reservoir, and the siphon pipes are used for the water to flow from the reservoir to irrigate cotton farms by gravity. Note that this paper does not discuss tailwater recovery. Therefore, the volume of irrigation water is the cotton planting water demand, and the water balance model in Section 2.2 is built based on these assumptions. One of the most popular RES in Australian cotton farms is solar PV [25]. Consequently, this study uses PV to build the GMG which allows excess energy to be fed back to the utility network. Fig. 1 shows the working architecture of the GMG in a cotton farm, where the MG river pump or MG bore pump means these pumps are all connected to MG, and the independent pump is the pump that cannot be connected to the MG, but connected to the grid directly. The IMG can be built by PV, battery storage, diesel generator, and a dummy load, where the dummy loads refer to loads that can consume excess energy to balance the generation-load relation. The excess energy can be stored by battery storage or absorbed by the dummy load. Fig. 2 illustrates the working structure of the IMG in a cotton farm, where the load is made of the dummy load, MG pumps powered by the MG, and the independent pumps driven by a diesel motor directly. The MPC methodology has an excellent performance in predictive control and handling uncertainties, which is suitable for cotton farms challenged with climate change and operational cost reduction and therefore adopted in this study. As for uncertainty modelling, the scenario-based approach is utilized to generate and reduce scenarios based on historical data, thereby building the stochastic model.

2.1. Power balance model of grid-connected microgrid

This section considers the GMG, which consists of only PV. The power balance can be represented as (1), and Eq. (2) represents the total PV power based on installed PV panel numbers [9].

$$P_{solar}(t,s) + P_{grid}(t,s) = \sum_{i=1}^{K} x_i(t,s) \times P_{pump,i}^{MG} + P_{fi}(t,s) \tag{1}$$

$$P_{solar}(t,s) = \sigma \times P_{solar}^{panel}(t,s) \tag{2}$$

s.t.

$$0 \le P_{grid}(t,s) \le \xi(t,s) \times P_{pump}^{total} \tag{3}$$

$$0 \le P_{fi}(t,s) \le [1-\xi(t,s)] \times P_{fi}^{max} \tag{4}$$

where σ denotes the installed PV panel units; $\xi(t,s) = 1$ means that MG purchases energy from the grid (import) at time t in scenario s, and $\xi(t,s) = 0$ means the MG sells energy to the grid (export) at time t and scenario s. Eqs. (3) and (4) represent the constraints that power purchase from the grid and feed-in to the grid cannot happen at the same time.

2.2. Power balance model of islanded microgrid

An IMG consists of PV, diesel generators, and battery storage. Due to the remote location of cotton farms, the cost of connecting to the grid is too high. Therefore, a common solution is using diesel generators as a backup energy source to build an IMG with renewable energy. The battery storage can help save diesel fuel during the irrigation period by storing excess energy, while the dummy load is used to consume the excess energy if the battery is full. Therefore, the power balance can be established as in (5).

$$\sum_{i=1}^{K} x_i(t,s) \times P_{pump,i}^{MG} + P_{charge}(t,s) + P_{dum}(t,s) = P_{solar}(t,s) + P_{diesel}(t,s) + P_{discharge}(t,s) \tag{5}$$

where, P_{charge} and $P_{discharge}$ represent the charge and discharge power of the battery storage, respectively; $P_{dum}(t,s)$ is a dummy load at time t and scenario s used to consume the excess energy when the battery is fully charged.

2.3. Battery model for islanded microgrid

In the IMG system, storing and utilizing excess renewable energy can save operational costs. In this study, the low-cost lead–acid battery is considered for energy storage systems, and the degradation cost is compared with its energy cost saving. Battery charging and discharging

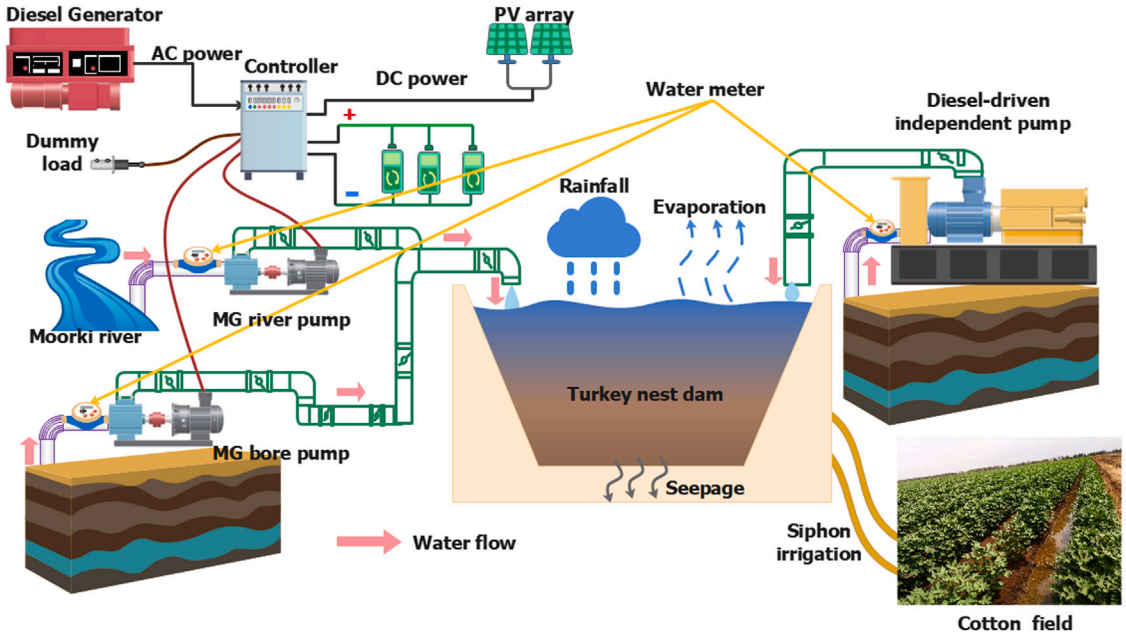

Fig. 2. Islanded cotton farm microgrid and pumping water system.

can be decided by several parameters, e.g., battery capacity B_{cap} (kWh), charging and discharging efficiency η_c and η_d. Eq. (6) illustrates the SOC model, and Eqs. (7)–(9) list the SOC limits and the constraint that charging cannot happen at the same time as discharging. On the other hand, a battery can store energy, but charging and discharging also cause battery degradation. See Appendix A for the battery degradation equations. Eqs. (A.1) – (A.2) show the Lead–acid battery storage degradation cost function f_{deg}, which is based on degradation coefficient κ_d [26].

$$S^{SOC}(t+1,s) = S^{SOC}(t,s) + \frac{P_{charge}(t,s)\times\eta_c\times\Delta t}{B_{cap}} - \frac{P_{discharge}(t,s)\times\Delta t}{B_{cap}\times\eta_d} \quad (6)$$

s.t.

$$S^{SOC}_{min} \le S^{SOC}(t,s) \le S^{SOC}_{max} \quad (7)$$

$$0 \le P_{charge}(t,s) \le \xi_B(t,s)\times P^{max}_{charge} \quad (8)$$

$$0 \le P_{discharge}(t,s) \le [1-\xi_B(t,s)]\times P^{max}_{discharge} \quad (9)$$

where Δt is the time interval, $\Delta t = 1$ h in this study; S^{SOC}_{max} and S^{SOC}_{min} denote the maximum and minimum SOC, respectively; Here, S^{SOC}_{min} = 10% and S^{SOC}_{max} = 100%. P^{max}_{charge} *and* $P^{max}_{discharge}$ are the charge or discharge limit of the battery storage; K_c is the number of the life cycle at the rated depth of discharge (DoD), and α (%) is DoD of the battery system.

2.4. Water balance model during the irrigation period

The pumps pump water from the bore/river into the reservoir during the cotton irrigation period, and the form of energy changes from electrical to potential energy. Farmers irrigate cotton fields with water from the reservoir by gravity. Therefore, the water balance is established by the reservoir's volume of water inflow and outflow. See Appendix B for the water balance equations. Eq. (B.1) defines the water balance in the reservoir; the water inflow and outflow are considered. Eq. (B.2) calculates the total water volume out from the reservoir. where W (ML) is the total water volume of the reservoir; W_{inflow} (ML) and $W_{outflow}$ (ML) represent the water inflow from and outflow volume to the reservoir; W_{see} (ML) is the value of average annual seepage from the reservoir, which is 10% of the reservoir capacity [27]. In the GMG, all the pumps (including MG and independent pumps) are electric. In the IMG, the MG pumps are electric, while the independent pumps are all diesel pumps. Equations (B.3) with the constraint (B.4) deal with the water inflow W_{inflow} for GMG and IMG, respectively. Also, the daily water usage limit W^{daily}_{max} (ML) [28] for GMG and IMG are expressed by (B.5) with the constraint (B.6). Eq. (B.7) establishes a constraint on the maximum amount of water that can be pumped by each independent pump in a day, where T is the prediction horizon (e.g., 24 h); $\varepsilon_{con,i} = \varepsilon^{in}_{con,i}$ = 4.55 kWh/ML/mTDH is the electricity consumed for lifting 1 ML water to 1-metre TDH [29,30]; h_i and h^{in}_i (mTDH) are the THD of the ith MG pump and independent pump, respectively. When$T$=24 h, W^{daily}_{max} is the maximum amount of water that can be pumped in a day by all the pumps; $V^{in}_{diesel,i}$ denotes the hourly fuel consumption of ith independent diesel-driven pump in IMG (L/h). $B^{MG,daily}_{i,max}$ and $B^{in,daily}_{i,max}$ (ML) denote the maximum amount of water that can be pumped by the ith MG pump and independent pump in a day, respectively.

2.5. Objective functions

The objective is to reduce the operational cost of the MG. The operational cost of GMG and IMG are defined in (10) and (11), respectively.

$$Y(t,s) = \left[P_{grid}(t,s) + \sum_{i=1}^{K} x^{in}_i(t,s)\times P^{in}_{pump,i}\right] \times\Delta t\times\beta_{buy}(t) - P_{fi}(t,s)\times\Delta t\times\beta_{sell}(t), \text{for GMG} \quad (10)$$

$$Y(t,s) = \left[P_{diesel}(t,s)\times\psi + \sum_{i=1}^{K^{in}} x^{in}_i(t,s)\times V^{in}_{diesel,i}\right] \times\Delta t\times\beta_{diesel}(t) + f_{deg}(t,s), \text{for IMG} \quad (11)$$

where $\beta_{buy}(t)$ and $\beta_{sell}(t)$ (AU$/kWh) represent the tariff of purchasing energy from the grid and the feed-in tariff of selling energy to the grid at the tth time, respectively; $\beta_{diesel}(t)$ indicates the diesel price at the tth time, and ψ is the electricity to diesel conversion coefficient.

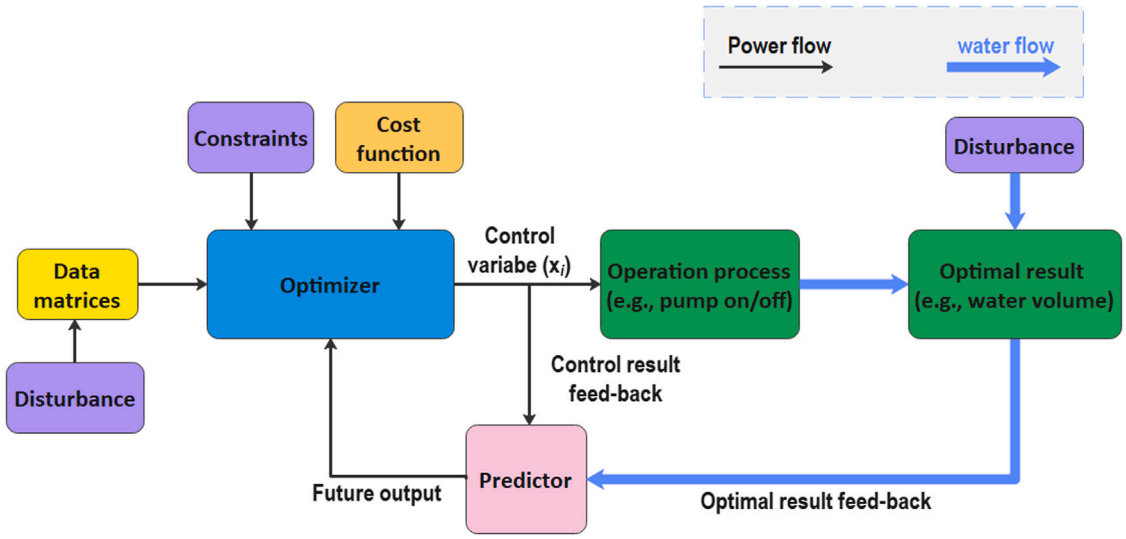

Fig. 3. Closed-loop MPC model.

2.6. MPC methodology

In order to obtain the result of minimizing the operational cost, the first step is to optimize the operational cost in a prediction horizon (T) (e.g., 24 h) with the open-loop optimization model (12) by considering all the typical scenarios.

$$\min_{x_i, x_i^{ind}} \sum_{s=1}^{Z} \sum_{t=1}^{T} \lambda_s \times Y(t,s) \quad t = 1, \ldots, T \quad s = 1, \ldots, Z \tag{12}$$

where, λ_s represents the probability of the scenario set s after scenario reduction; and Z is the number of the typical scenarios. In addition, the closed-loop MPC model (13) is based on (12) and moving the prediction horizon to the next interval with periodically updated system information to provide feedback to the controller. Fig. 3 shows the closed-loop MPC concept in this study.

$$\min_{x_i, x_i^{ind}} \sum_{s=1}^{Z} \sum_{t=1+m}^{T+m} \lambda_s \times Y(t,s) \tag{13}$$

where the period $[1 + m, \ldots, T + m]$ is the window of moving prediction horizon.

2.7. Scenario-based model

This paper proposes scenario-based techniques to deal with uncertainty datasets for the MG system. Firstly, the uncertainties affecting the operational costs of pumping water on the cotton farm need to be determined, e.g., RES in the power balance model, precipitation, evaporation, and irrigation demand in the water balance model. Two scenario-based uncertainty models are proposed to process the above-mentioned uncertainties: the static and dynamic scenario-based uncertainty models. In the static uncertainty model, all uncertainty datasets during the entire irrigation period are used only once for scenario generation and reduction, and the resultant typical scenarios are fixed for all the MPC iterations. The computation time of this uncertainty model is less as the scenario generation and reduction only needs to be conducted once in the whole MPC time horizon, while the uncertainty representation accuracy is sacrificed. Fig. 4 shows the static scenario-based MPC optimization flowchart. As shown, the flowchart begins with forming uncertainty datasets represented in matrix form. All the uncertain datasets formed by matrices are input to the SCENRED toolbox, where the scenario generation and reduction process are completed. This step is crucial for managing the inherent uncertainties in RESs, ensuring the MPC can effectively optimize the operation under varying scenarios. Then, the static typical scenarios with their corresponding probability are sent to the MPC solver and used in all the MPC iterations to obtain the optimal operational cost results.

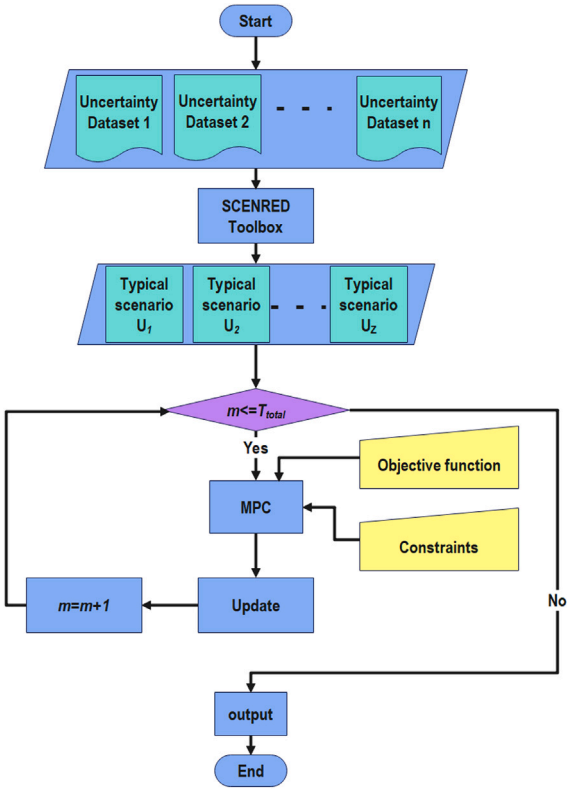

Fig. 4. Static scenario-based MPC model.

In the dynamic scenario-based uncertainty model, within each moving time horizon, the future period in close proximity T^{scen} (e.g., ten days or fortnight into the future) can be chosen with the available historical data. Therefore, the corresponding typical scenarios after scenario generation and reduction are dynamically updated within each

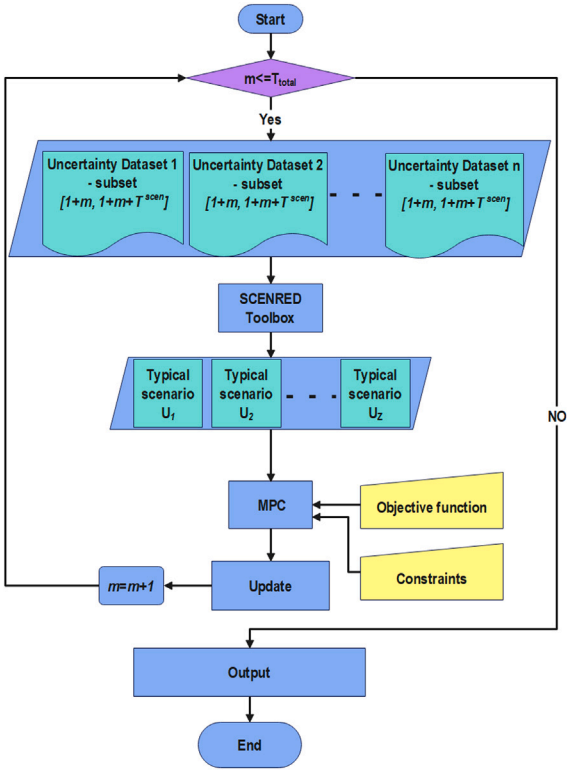

Fig. 5. Dynamic scenario-based MPC model.

MPC iteration. The dynamic scenario-based model is more accurate as it uses the data in close proximity to generate the typical scenarios; however, the computation time may be an issue due to the necessity of scenario generation and reduction within each moving time horizon. Fig. 5 illustrates the dynamic scenario-based MPC optimization process. The scenario generation and reduction are updated within each MPC iteration, and the typical scenarios are continuously updated.

In summary, the difference between the static and the dynamic scenario-based uncertainty models is that the static one obtains the scenarios once for all; while the dynamic case needs to update the typical scenarios for the entire process continuously.

3. Case study

To simulate the proposed scenario-based stochastic MPC approach for the cotton farm MG, the cotton farm information based on [23] from a real cotton farm located in Gunnedah, New South Wales, Australia, is used. In this study, the corresponding historical data are utilized for the irrigation period of 87 days spanning from early November 2016 to the end of February 2017. This is because cotton needs massive amounts of water only in the growing season, which is the summer season (November to February) in Australia in the southern sphere [31]. Five different cases are adopted to compare the results and demonstrate the applicability of the approach, which include Baseline case and standard MPC, static scenario-based MPC for GMG, dynamic scenario-based MPC for GMG, static scenario-based MPC for IMG, and dynamic scenario-based MPC for IMG.

- Case 1: Baseline case and standard MPC.
  The Baseline case is that farmers manually control all pumping systems based on their irrigation experience, and they can also obtain future weather information from the Bureau of Meteorology (BOM) or local weather stations. Fig. 1 demonstrates the GMG's equipment layout and irrigation mode in the study cotton farm.

Table 1
System parameters of the GMG in the cotton farm.

Items	Values
MG bore Pump #1 ($P^{MG}_{pump,1}$)	75 kW
MG river Pump #2 ($P^{MG}_{pump,2}$)	37 kW
Independent bore Pump #1 ($P^{in}_{pump,1}$)	75 kW
Farm area	3 $\times 10^6$ m^2
Bore pump head (h_1 or h^{in}_1)	31 mTDH
River pump head (h_2)	12 mTDH
Average energy for lifting 1 ML/mTDH (ϵ_{con})	4.55 kWh/ML/mTDH
Average water demand (W_{irr})	6.5 $\times 10^{-4}$ ML/m^2
Maximum allowed water usage	1800 ML/year
Reservoir capacity	800 ML
Average hourly seepage ($W_{see}/(24 \times 365)$)	4.56 m^3/h
Installed solar PV capacity ($\sigma \times P^{panel}_{solar}$)	50.6 kW
Fixed-rate tariff in 2016 (β_{buy})	0.26 AU$/kWh
FIT in 2016 (β_{sell})	0.06 AU$/kWh

Table 2
The details of the pump operation in the Baseline case in 2016.

	Values
MG bore Pump #1 work hours	1034 h
MG river Pump #2 work hours	882 h
Independent bore Pump #1 work hours	360 h
MG bore Pump #1 usage	75,812.33 kWh
MG river Pump #2 usage	63,551.06 kWh
Independent bore Pump #1 usage	12,865.24 kWh
Total operational cost	AU$ 39,580
Total pumped water	1223.6 ML

Table 3
Operational results of Baseline case and standard MPC [9].

Microgrid items	Operational cost (AU$)	Total pumped water (ML)
GMG Baseline	39,580	1224
GMG MPC	27,556	1181
IMG Baseline	40,902	1181
IMG MPC	31,164	1178

Table 1 lists the corresponding system parameters in Fig. 1 [32]. Based on [9], the breakdown energy cost of the Baseline case is listed in Table 2. The standard MPC approach in [9] discusses the operational cost of the studied cotton farm, but the method only caters to the microgrid energy dispatch scenarios and does not focus on uncertainty modelling. For a comparison of the current study, the Baseline and standard MPC results are shown in Table 3.

- Case 2: Static scenario-based MPC for GMG
  In this case, the static scenario generation and reduction from Section 2.7 are used to obtain ten sets of typical scenarios and their corresponding probability, derived from the 87-day historical data. For the operational cost optimization, ten typical scenarios are substituted into (12). At last, the closed-loop MPC of (13) with a prediction horizon of 24 h is used to obtain each pump's operation status and the operational cost of the entire irrigation period.
- Case 3: Dynamic scenario-based MPC for GMG
  The simulation is based on the dynamic scenario-based uncertainty model in Section 2.7, which uses the historical data of 14 days ahead of the current time instant. For this study, both the static and dynamic scenario-based MPC approaches are compared, using the same historical data. The differences between the static and dynamic scenario-based approaches are that in the dynamic one, ten typical scenarios are obtained based on the moving 14-day datasets, and the obtained ten typical scenarios will be updated at each MPC iteration whenever the optimization horizon changes.

Table 4
System parameters of the IMG in the studied cotton farm [34].

Items	Values
Diesel conversion coefficient (ψ)	0.2695 L/kWh
Diesel consumption for lifting 1ML/m water (δ_{diesel})	1.1 L/ML/mTDH
Unit price of diesel in 2016 (after subsidy) (β_{diesel})	AU$ 1.15 /L
Lead–acid battery capacity (B_{cap})	25 kWh
Lead–acid battery cost (C_{Bat})	AU$ 2750
Charge/discharge efficiencies (η_c or η_d)	90%
Charge/discharge limit ($P^{max}_{charge}/P^{max}_{discharge}$)	15 kWh
Lead–acid battery life cycle ($K_c \times \alpha$)	2000 @ 60% DoD

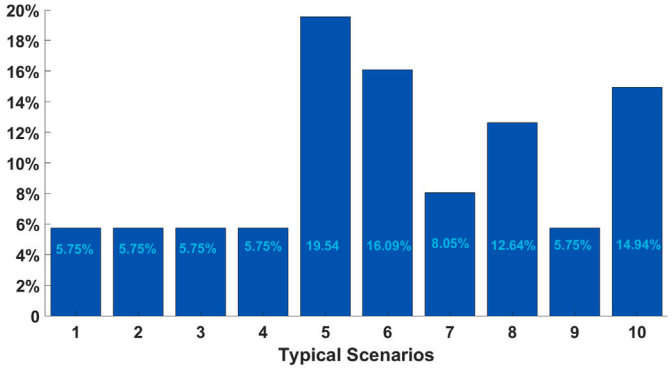

Fig. 6. Probability of static typical scenarios.

- Case 4: Static scenario-based MPC for IMG
  Many cotton farm pumping sites in Australia are far from the grid [33]. IMGs using diesel generators, solar energy, and lead–acid battery storage are widely built on cotton farms. Based on the previous MPC study for IMG [9], the IMG of the studied cotton farm is shown in Fig. 2, with the system parameters in Table 4. Then, the historical data of the studied cotton farm in 2016 are substituted, and the algorithm proposed in Section 2.7 is adopted. The pump operation during the entire irrigation period can be optimized for the IMG system. Also, the operation cost under uncertainties can be obtained.
- Case 5: Dynamic scenario-based MPC for IMG
  Dynamic scenario generation and reduction are applied for IMG using the model in Section 2.7, and then the operational cost and each pump's action can be obtained by the underlying stochastic MPC methodology. In order to compare both the static and dynamic scenario-based MPC, the same cotton farm's historical data are used.

4. Results and discussions

This section discusses the key results of MPC for cotton farm MG under uncertainties. Scenario generation and reduction methodology are employed to simulate four different cases (cases 2–5), and the results from each case are analysed and compared to the Baseline case.

4.1. Static scenario generation and reduction

In this study, the cotton farm data during the irrigation period of 2016–2017 include historical solar generation data, rainfall data [35], hourly evaporation data of the cotton farm area [36] and the cotton life-cycle water demand data. Each typical scenario has its corresponding probability, as shown in Fig. 6. For the entire irrigation period, scenario generation and reduction can be illustrated in Figs. 7(a) and 7(b), respectively.

Table 5
Operational result comparison of grid-connected microgrid.

	Operational cost (AU$)	Total pumped water (ML)
Baseline case	39,580	1224
Standard MPC	27,556	1181
Static scenario-based MPC	22,595	1233
Dynamic scenario-based MPC	18,797	1238

4.2. Dynamic scenario generation and reduction

In the dynamic scenario generation and reduction method, the two-week data ahead of the current time instant are taken to produce ten typical scenarios. For instance, Figs. 8(a) and 8(b) show the evaporation curves before and after scenario generation and reduction methodology in 4 consecutive MPC iterations.

4.3. Scenario-based MPC operation results for grid-connection microgrid

With the help of the scenario generation and reduction method for the historical dataset, the closed-loop MPC is implemented to optimize the operation of each pump during the whole irrigation period. The hourly control variables (x_i and x_i^{in}) can be obtained by solving (10) and (13). Fig. 9(a) shows the on/off status of MG bore pump #1 (turned on for 1125 h), MG river pump #2 (turned on for 810 h) and the independent pump #1 (turned on for 176 h), which are controlled under the static scenario-based MPC. Fig. 9(b) shows the pump's on/off status under the dynamic scenario-based MPC, where MG bore pump #1 worked for 1031 h, MG river pump #2 worked for 1137 h, and the independent pump #1 worked for 76 h. It can be observed from Fig. 9 that the usage rate of the water pumps connected to the MG is higher than the independent pump. The utilization rate of the independent pump in the static scenario-based MPC is slightly higher than that in the dynamic scenario-based MPC. Table 5 shows the comparison of the proposed scenario-based MPC with the Baseline case and the standard MPC. The expected value of the operational cost for static scenario-based MPC is AU$ 22,595, which saves AU$ 16,985 compared with the Baseline case and saves AU$ 4961 compared with the standard MPC. Moreover, the expected operational cost value of the dynamic scenario-based MPC is AU$ 18,797, which is AU$ 20,783 less than the Baseline case and AU$ 8759 less than the standard MPC.

4.4. Scenario-based MPC operation results for islanded microgrid

To verify that the proposed approach is also suitable for IMG, the same cotton farm parameters are assumed for the IMG with diesel generators as a backup power source, and a 25 kWh lead–acid battery storage is equipped to store the excess energy. The scenario generation and reduction processes use the same dataset to facilitate the comparison with the Baseline case and the standard MPC for IMG. Based on (11) and (13), the pump control variables can be obtained and listed in Table 6. In addition, Table 7 shows the results of total pumped water volume and the operational cost for each IMG case. The expected value of operational cost from the static scenario-based MPC is AU$ 13,486 lower than the Baseline case and AU$ 3748 lower than the standard MPC. For the dynamic scenario-based MPC, it has the lowest operational cost value AU$ 24,443, which is AU$ 16,459 lower than the Baseline case and AU$ 6721 lower than the standard MPC. In the IMG system, the excess electrical energy is stored in the batteries and released to the pumps when needed. According to the battery pack

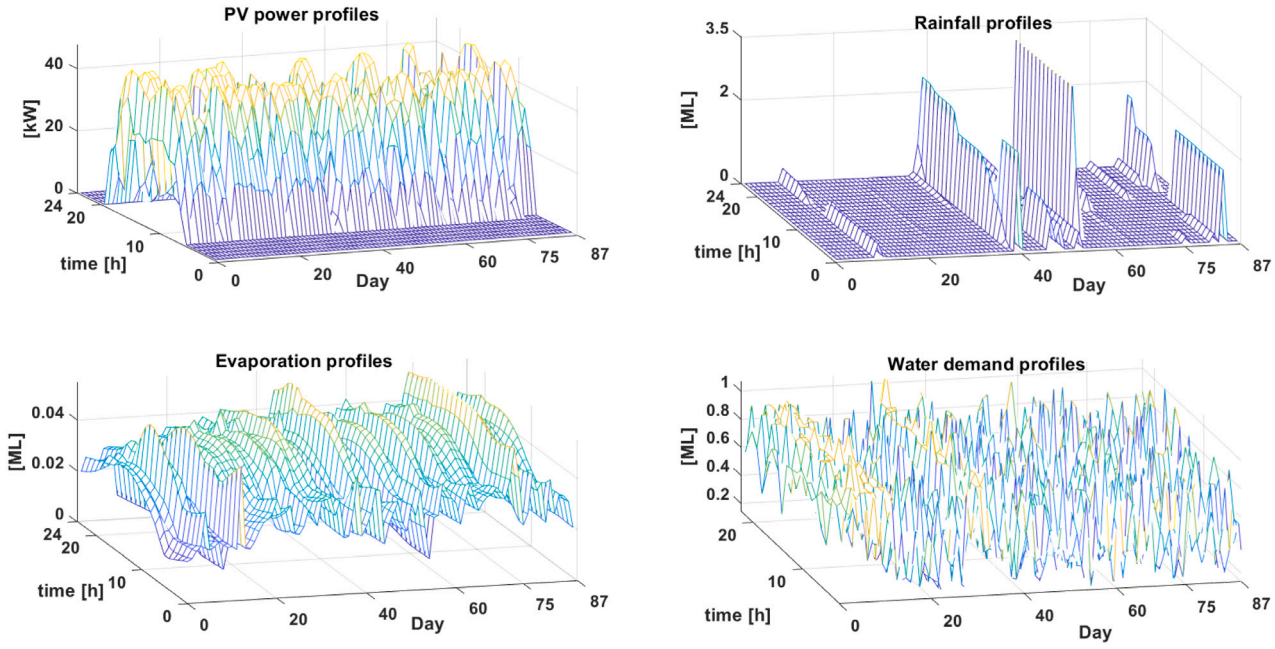

(a) Uncertainty data for the entire irrigation period

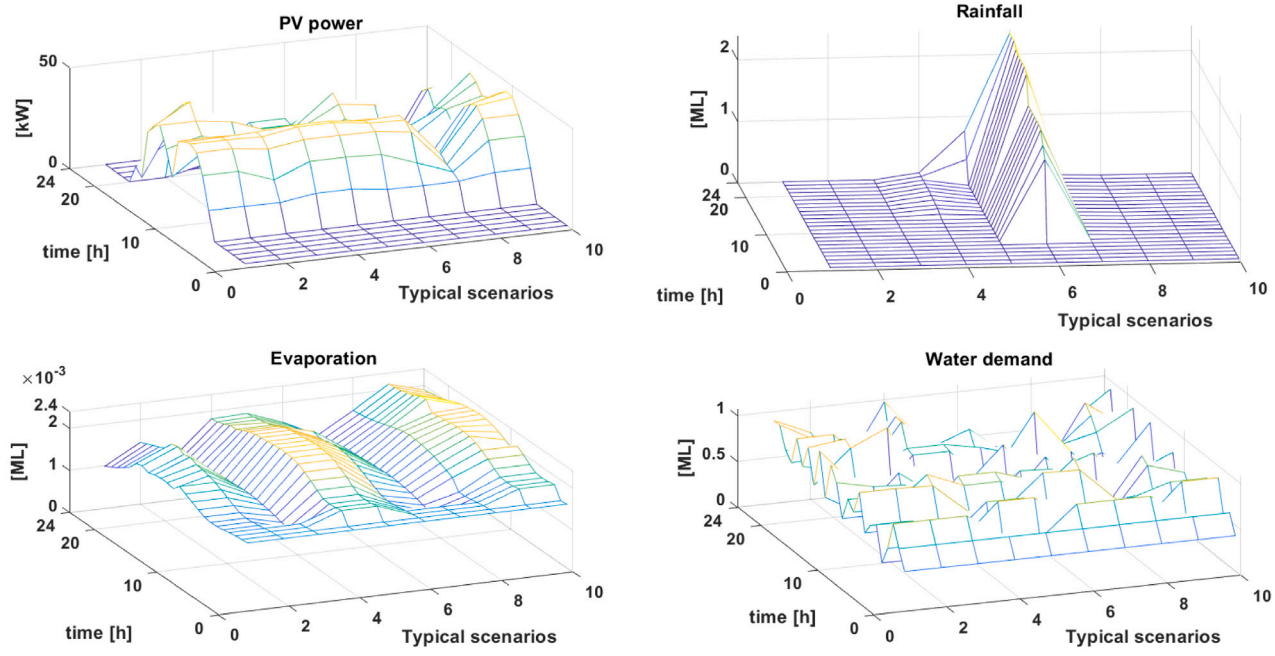

(b) Ten typical scenarios after reduction

Fig. 7. Static scenario generation and reduction for the studied cotton farm.

parameters in Table 4, and the methodology in Section 2.3, the battery pack usage during the entire irrigation period can be obtained. Fig. 10 shows the battery charging and discharging pattern for the static and dynamic scenario-based MPC. Meanwhile, Table 8 lists the operational results of the battery storage. It can be observed from Fig. 8 that the dynamic scenario-based MPC generates ten typical scenarios for each MPC iteration, and thus, the role of batteries is clearly reflected in the MG. The battery pack for the dynamic scenario-based MPC can reuse 821 kWh of excess energy to power the MG pumps. During the entire irrigation period, the energy cost savings from utilizing the battery storage is AU$ 87.24 more than the cost of battery pack degradation under the dynamic scenario-based MPC, which means using the battery to store and reuse the excess energy from the RES can save the operational cost of AU$ 87.24.

4.5. Robustness analysis and performance comparison

In this part, the proposed Scenario-based MPC approach integrates a mechanism for detecting the robustness range, aiming to identify the proportion of "bad" data that the system can tolerate. This feature is pivotal in ensuring the resilience of the control system against unexpected disturbances or sensor inaccuracies. Assuming a number of bad data (zeros) are injected into the dataset (e.g., sensor intermittence or missing data), a maximum tolerance is needed to know when the

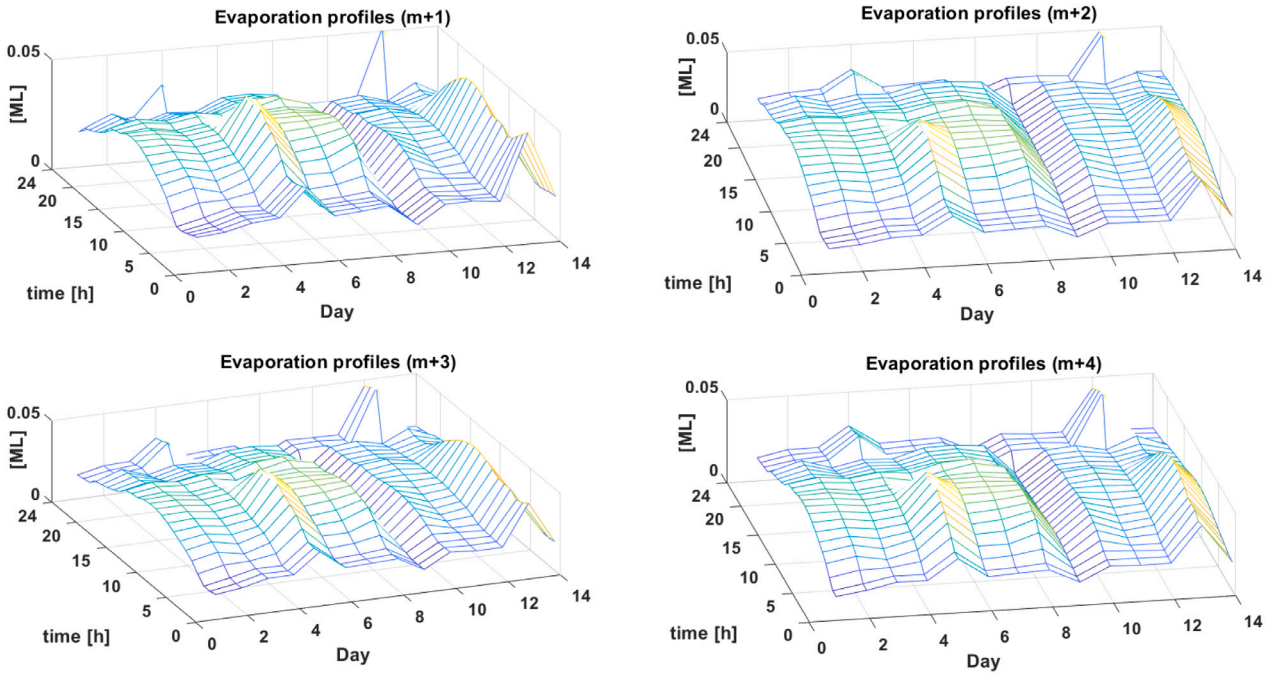

(a) 14-day evaporation data

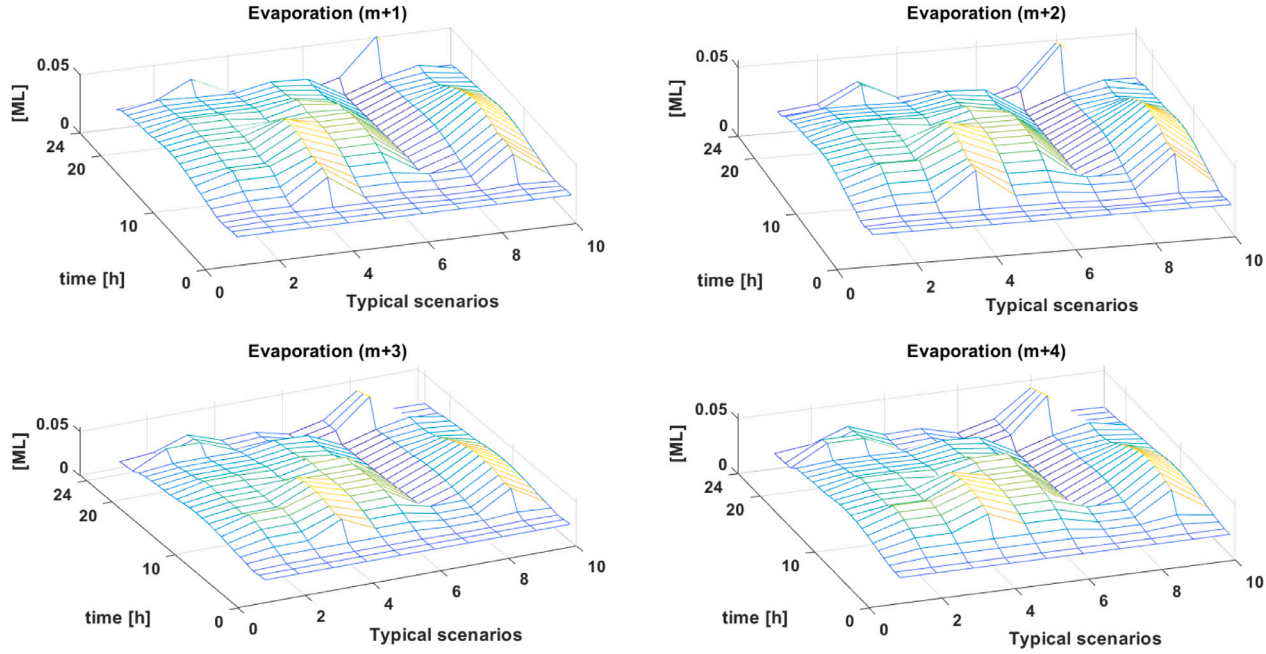

(b) Ten evaporation typical scenarios after reduction in 4 consecutive MPC iterations

Fig. 8. Dynamic scenario generation and reduction by using the future 14-day data.

Table 6
Pump's operational results of the scenario-based MPC for islanded microgrid.

	Operation hours (h)	Pumped water (ML)
Static x_1	515	274
Static x_2	995	647
Static x_1^{in}	493	262
Dynamic x_1	381	203
Dynamic x_2	1094	741
Dynamic x_1^{in}	507	270

Table 7
Operational result comparison of islanded microgrid.

	Operational cost (AU$)	Total pumped water (ML)
Baseline case	40,902	1181
Standard MPC	31,164	1178
Static scenario-based MPC	27,416	1214
Dynamic scenario-based MPC	24,443	1210

typical scenarios start to change. Table 9 shows the maximum percentage of bad data for each variable in the dataset. From Table 9,

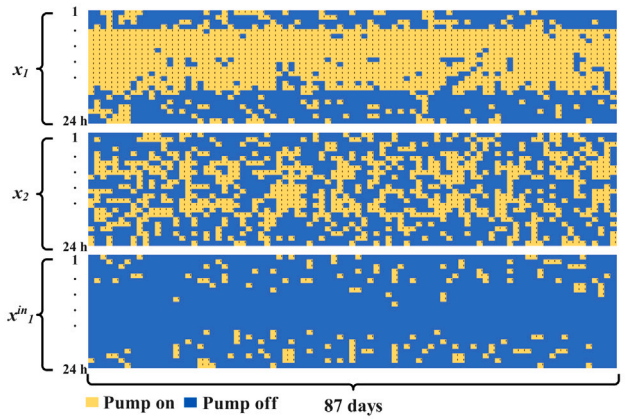

(a) Pump's on/off status under static scenario-based MPC

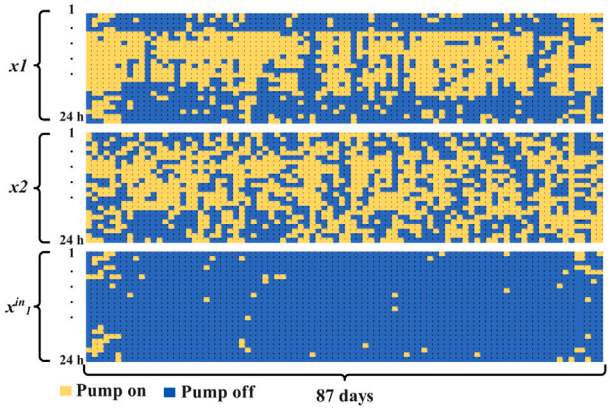

(b) Pump's on/off status under dynamic scenario-based MPC

Fig. 9. Pump's on/off status for grid-connected microgrid.

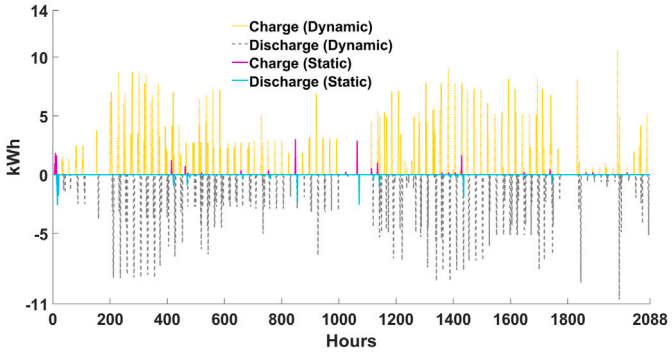

Fig. 10. Battery charging and discharging pattern in islanded microgrid.

Table 8
Operational results of the battery storage.

	Static scenario	Dynamic scenario
Energy charge (kWh)	31.53	821.77
Energy discharge (kWh)	33.42	821.56
Saved cost (AU$)	10.35	254.62
Degradation cost (AU$)	6.61	167.38

the Water Demand variable exhibits the highest sensitivity, with a tolerance of 4.50%, indicating that up to 94 zeros (i.e., bad data) can be accommodated without adversely affecting the outcome. On the other hand, the Rainfall variable demonstrates a sensitivity of 17.19%, implying that the method's outcomes remain unaffected with 359 bad data.

Table 9
Bad data tolerance of each variable in the dataset.

Variable	Bad data tolerance (%)
Solar	9.53
Rainfall	17.19
Evaporation	9.48
Water Demand	4.50

Table 10
Comparison results of static scenario-based MPC and the optimization method in [3].

	Operational cost (AU$)	*Running time (h)
Static scenario-based MPC	27,416	9.1
Gradient-based optimization in [3]	36,425	56.15

* MATLAB 2022a, i7-8650U CPU @ 2.11 GHz and 16G RAM

Next, the method from [3] and the proposed MPC method in this paper are compared in this section. In (12), the prediction horizon T spans the entire irrigation period (e.g., 2088 h). The solver in [3] utilizes gradient-based optimization tools in Matlab to solve the operational cost minimization problem of the cotton farm microgrid. For simplicity, MATLAB's fmincon function is used to solve constrained multi-objective nonlinear optimization problems. Table 10 provides an assessment of the operational cost and computing time for both optimization methods. It can be seen that the proposed MPC method has significant operational cost savings because the decisions are made based on predicted future condition changes. In terms of computational time, the MPC method requires only one-sixth of the time needed by the gradient-based optimization method in [3].

5. Conclusion

This study proposes two scenario-based approaches to model the uncertainties of environmental and demand factors on cotton farms by scenario generation and reduction under the MPC framework. Then, the MPC method is used to optimize the operation of the MG and cotton farm water pump under the typical scenarios for the underlying uncertainties. The proposed method is validated by case studies on a cotton farm. It is found that the operational cost of the static and dynamic scenario-based MPC for the GMG are AU$ 22,595 and AU$ 18,797, which are AU$ 4961 and AU$ 8759, respectively, lower than that of the standard MPC. For the IMG, the operational cost of static and dynamic scenario-based MPC are AU$ 3748 and AU$ 6721, sequentially, lower than the standard MPC. By utilizing the robustness detection method, the proposed scenario generation and reduction can tolerate 17.19% and 4.5% bad data of rainfall and water demand, respectively. Additionally, based on the comprehensive evaluation of static scenario-based MPC and gradient-based optimization tools, considering both performance and practical constraints, it is shown that the proposed methodology is more suitable for the cotton farm microgrid application.

In future work, the static scenario-based MPC approach for cotton farm MG control systems will use more years of historical data to improve its reliability. For the dynamic scenario-based MPC approach, an investigation will be conducted on how to reduce the computation burden for real-time implementations. Also, the integration of AI and machine learning techniques is planned to refine scenario-based MPC approaches. These technologies offer more accurate predictions of environmental and operational variables. Specifically, machine learning algorithms will be employed to analyse historical data more effectively, allowing better handling of uncertainties and bad data. AI and machine learning techniques can significantly improve both the static and dynamic scenario-based MPC approaches, ultimately contributing to more cost-effective and reliable MG operations on cotton farms.

CRediT authorship contribution statement

Yunfeng Lin: Writing – original draft, Software, Methodology. **Li Li:** Writing – review & editing, Supervision, Software, Project administration, Conceptualization. **Jiangfeng Zhang:** Writing – review & editing, Validation, Supervision, Formal analysis, Conceptualization. **Jiatong Wang:** Writing – review & editing, Software.

Declaration of competing interest

We wish to confirm that there are no known conflicts of interest associated with this publication and there has been no significant financial support for this work that could have influenced its outcome.

Data availability

Data will be made available on request.

Acknowledgements

This study is funded by the Cotton Research and Development Corporation (CRDC), Australia and supported by an Australian Government Research Training Program scholarship, Australia.

Appendix A. Battery degradation equations

$$\kappa_d = \frac{C_{Bat}}{B_{cap} \times \eta_d \times K_c \times \alpha} \tag{A.1}$$

$$f_{deg}(t,s) = P_{charge}(t,s) \times \Delta t \times \kappa_d + P_{discharge}(t,s) \times \Delta t \times \kappa_d \tag{A.2}$$

Appendix B. Water balance equations

$$W(t+1,s) = W(t,s) + W_{inflow}(t,s) - W_{outflow}(t,s) \tag{B.1}$$

$$W_{outflow}(t,s) = W_{irr}(t,s) + W_{eva}(t,s) + \frac{W_{see}}{24 \times 365} \tag{B.2}$$

$$\begin{cases} W_{inflow}(t,s) = \sum_{i=1}^{K} \frac{x_i(t,s) \times P_{pump,i}^{MG} \times \Delta t}{\epsilon_{con,i} \times h_i} + \sum_{i=1}^{K^{in}} \frac{x_i^{in}(t,s) \times P_{pump,i}^{in} \times \Delta t}{\epsilon_{con,i}^{in} \times h_i^{in}} + W_{R\_res}(t,s), \\ \text{(GMG water inflow)} \\ W_{inflow}(t,s) = \sum_{i=1}^{K} \frac{x_i(t,s) \times P_{pump,i}^{MG} \times \Delta t}{\epsilon_{con,i} \times h_i} + \sum_{i=1}^{K^{in}} \frac{x_i^{in}(t,s) \times V_{diesel,i}^{in} \times \Delta t}{\delta_{diesel,i}^{in} \times h_i^{in}} + W_{R\_res}(t,s), \\ \text{(IMG water inflow)} \end{cases} \tag{B.3}$$

s.t.

$$x_i(t,s) \ (or \ x_i^{in}(t,s)) = \begin{cases} 1, & \text{when the } i\text{th pump is on} \\ 0, & \text{when the } i\text{th pump is off} \end{cases} \tag{B.4}$$

$$\begin{cases} \sum_{t=1}^{T} \left(\sum_{i=1}^{K} \frac{x_i(t,s) \times P_{pump,i}^{MG} \times \Delta t}{\epsilon_{con,i} \times h_i} + \sum_{i=1}^{K^{in}} \frac{x_i^{in}(t,s) \times P_{pump,i}^{in} \times \Delta t}{\epsilon_{con,i}^{in} \times h_i^{in}} \right) \\ \le W_{max}^{daily}, \ \text{GMG water daily limit for all pumps} \\ \sum_{t=1}^{T} \left(\sum_{i=1}^{K} \frac{x_i(t,s) \times P_{pump,i}^{MG} \times \Delta t}{\epsilon_{con,i} \times h_i} + \sum_{i=1}^{K^{in}} \frac{x_i^{in}(t,s) \times V_{diesel,i}^{in} \times \Delta t}{\delta_{diesel,i}^{in} \times h_i^{in}} \right) \\ \le W_{max}^{daily}, \ \text{IMG water daily limit for all pumps} \end{cases} \tag{B.5}$$

s.t.

$$\sum_{t=1}^{T} \left(\frac{x_i(t,s) \times P_{pump,i}^{MG} \times \Delta t}{\epsilon_{con,i} \times h_i} \right) \le B_{i,max}^{MG,daily} \tag{B.6}$$

$$\begin{cases} \sum_{t=1}^{T} \left(\frac{x_i^{in}(t,s) \times P_{pump,i}^{in} \times \Delta t}{\epsilon_{con,i}^{in} \times h_i^{in}} \right) \le B_{i,max}^{in,daily}, \\ \text{(GMG water daily limit for each independent pump)} \\ \sum_{t=1}^{T} \left(\frac{x_i^{in}(t,s) \times V_{diesel,i}^{in} \times \Delta t}{\delta_{diesel,i}^{in} \times h_i^{in}} \right) \le B_{i,max}^{in,daily}, \\ \text{(IMG water daily limit for each independent pump)} \end{cases} \tag{B.7}$$

References

[1] Foley JP, Sandell GR, Szabo PM, Baillie CP. Improving energy efficiency on irrigated Australian cotton farms updated june 2015. Technical report, CottonInfo; 2015.

[2] Cottoninfo. Energy use efficiency. 2022, https://cottoninfo.com.au/energy-use-efficiency.

[3] Lin Yunfeng, Wang Jiatong, Zhang Jiangfeng, Li Li. Microgrid optimal investment design for cotton farms in Australia. Smart Grids Sustain Energy 2023;9(1):5.

[4] Wang Wei, Huang Yifan, Yang Ming, Chen Changyue, Zhang Yumin, Xu Xingming. Renewable energy sources planning considering approximate dynamic network reconfiguration and nonlinear correlations of uncertainties in distribution network. Int J Electr Power Energy Syst 2022;139:107791.

[5] Elkazaz Mahmoud, Sumner Mark, Thomas David. Energy management system for hybrid PV-wind-battery microgrid using convex programming, model predictive and rolling horizon predictive control with experimental validation. Int J Electr Power Energy Syst 2020;115:105483.

[6] Hu Jiefeng, Shan Yinghao, Guerrero Josep M, Ioinovici Adrian, Chan Ka Wing, Rodriguez Jose. Model predictive control of microgrids – An overview. Renew Sustain Energy Rev 2021;136:110422.

[7] Batiyah Salem, Sharma Roshan, Abdelwahed Sherif, Zohrabi Nasibeh. An MPC-based power management of standalone DC microgrid with energy storage. Int J Electr Power Energy Syst 2020;120:105949.

[8] Gu Wei, Wang Zhihe, Wu Zhi, Luo Zhao, Tang Yiyuan, Wang Jun. An online optimal dispatch schedule for CCHP microgrids based on model predictive control. IEEE Trans Smart Grid 2016;8(5):2332–42.

[9] Lin Yunfeng, Zhang Jiangfeng, Li Li. A model predictive control approach to a water pumping system in an Australian cotton farm microgrid. Clean Energy Syst 2022;3:100026.

[10] Kaut Michal, Wallace Stein. Evaluation of scenario-generation methods for stochastic programming. Pac J Optim 2003;3.

[11] Hø yland Kjetil, Wallace Stein W. Generating scenario trees for multistage decision problems. Manag Sci 2001;47(2):295–307.

[12] Aghaei Jamshid, Niknam Taher, Azizipanah-Abarghooee Rasoul, Arroyo José M. Scenario-based dynamic economic emission dispatch considering load and wind power uncertainties. Int J Electr Power Energy Syst 2013;47:351–67.

[13] Lee Jin-Oh, Kim Yun-Su. Novel battery degradation cost formulation for optimal scheduling of battery energy storage systems. Int J Electr Power Energy Syst 2022;137:107795.

[14] Yu Jiah, Ryu Jun-Hyung, Lee In-beum. A stochastic optimization approach to the design and operation planning of a hybrid renewable energy system. Appl Energy 2019;247:212–20.

[15] Luo Liang, Abdulkareem Sarkew S, Rezvani Alireza, Miveh Mohammad Reza, Samad Sarminah, Aljojo Nahla, Pazhoohesh Mehdi. Optimal scheduling of a renewable based microgrid considering photovoltaic system and battery energy storage under uncertainty. J Energy Storage 2020;28:101306.

[16] Mohammadi Sirus, Soleymani Soodabeh, Mozafari Babak. Scenario-based stochastic operation management of MicroGrid including wind, photovoltaic, microturbine, fuel cell and energy storage devices. Int J Electr Power Energy Syst 2014;54:525–35.

[17] Zhu Dinghuan, Hug Gabriela. Decomposed stochastic model predictive control for optimal dispatch of storage and generation. IEEE Trans Smart Grid 2014;5(4):2044–53.

[18] Farina Marcello, Giulioni Luca, Scattolini Riccardo. Stochastic linear model predictive control with chance constraints–a review. J Process Control 2016;44:53–67.

[19] Heirung Tor Aksel N, Paulson Joel A, O'Leary Jared, Mesbah Ali. Stochastic model predictive control—how does it work? Comput Chem Eng 2018;114:158–70.

[20] Shang Chao, You Fengqi. A data-driven robust optimization approach to scenario-based stochastic model predictive control. J Process Control 2019;75:24–39.

[21] Pippia Tomas, Lago Jesus, De Coninck Roel, De Schutter Bart. Scenario-based nonlinear model predictive control for building heating systems. Energy Build 2021;247:111108.

[22] Hans Christian A, Sopasakis Pantelis, Bemporad Alberto, Raisch Jörg, Reincke-Collon Carsten. Scenario-based model predictive operation control of islanded microgrids. In: 2015 54th IEEE conference on decision and control. IEEE; 2015, p. 3272–7.

[23] Lin Yunfeng, Zhang Jiangfeng, Li Li, Wang Jiatong. A model predictive control approach for cotton farm microgrid operation under uncertainties. In: 2022 32st Australasian universities power engineering conference. IEEE; 2022, p. 1–6.
[24] Growe-Kuska Nicole, Heitsch Holger, Romisch Werner. Scenario reduction and scenario tree construction for power management problems. In: 2003 IEEE Bologna power tech conference proceedings, vol. 3. IEEE; 2003, p. 7–pp.
[25] Chen Guangnan, Sandell Gary, Baillie Craig. Alternative energy sources for cotton production in Australia. In: Proceedings of the 18th world congress of the international commission of agriculture and biosystems engineering. University of Southern Queensland; 2014.
[26] Chen Tao, Su Wencong. Local energy trading behavior modeling with deep reinforcement learning. IEEE Access 2018;6:62806–14.
[27] Agriculture Victoria. Seepage losses from farm dams. 2021, https://calculator.agriculture.vic.gov.au/fwcalc/information/seepage-losses-from-farm-dams.
[28] NSW Government. Water access licences. 2021, https://www.dpie.nsw.gov.au/water/licensing-and-trade/licensing. (Retrieved 10 October 2022).
[29] Foley Joseph. Fundamentals of energy use in water pumping. Irrigation Aust Off J Irrigation Austr 2015;31(1):8–9.
[30] Jason Alexandra, Eyre N, Alexandra J, Richards R, Swann E. The water & energy nexus: A multi-factor productivity challenge. NSW Farmers Association; 2014.
[31] Cotton Australia. How is cotton grown? 2022, https://www.https://cottonaustralia.com.au/how-is-cotton-grown.
[32] Gerry Flores, David Hoffmann, Leigh Rostron, Shorten Phil. VSDs lead irrigation efficiency measures for Gunnedah cropping enterprise. 2013, https://www.pumpindustry.com.au.
[33] Australiaand Geoscience Australiaand Australian Bureau of Agricultural and Resource Economics. Australian energy resource assessment. 2014, xii, 344 p. : URL https://www.ga.gov.au/products/servlet/controller?event=GEOCAT_DETAILS&catno=70142. (Retrieved 30 October 2022).
[34] NSW Department of Primary Industries. Primefact- Comparing running costs of diesel, LPG and electrical pumpsets. 2016, https://www.dpi.nsw.gov.au/_data/assets/pdf_file/0011/665660/comparing-running-costs-of-diesel-lpg-and-electrical-pumpsets.pdf.
[35] Australian Government Bureau of Meteorology. Daily rainfall- Gunnedah Airport AWS. 2022, http://www.bom.gov.au/climate/data/stations/.
[36] Queensland Government. Open Data Portal - SILO climate database - evaporation - synthetic. 2022, https://www.data.qld.gov.au/dataset/silo-climate-database-evaporation-synthetic.